

# Giant magnetoresistance across the phase transition in spin crossover molecules

N. Baadji and S. Sanvito

*School of Physics and CRANN, Trinity College, Dublin 2, Ireland*

(Dated: April 29, 2022)

The electronic origin of a giant magnetoresistance effect in nanoscale junctions incorporating a spin crossover molecule is demonstrated theoretically by using a combination of density functional theory and the non-equilibrium Green's functions method for quantum transport. At the spin crossover phase transition there is a drastic change in the electronic gap between the frontier molecular orbitals. As a consequence, when the molecule is incorporated in a two terminal device, the current increases by about four orders of magnitude in response to the spin change. This is equivalent to a giant magnetoresistance effect in excess of 10,000 %. Since the typical phase transition critical temperature for spin crossover compounds can be extended to well above room temperature, spin crossover molecules appear as the ideal candidate for implementing spin devices at the molecular level.

PACS numbers:

The last few years have witnessed several attempts at implementing spin devices at the single molecule level [1–3]. These include spin-valves, where organic molecules are used as transport medium for spin-polarized electrons injected from magnetic metals [4–6], and three terminal junctions incorporating magnetic molecules [7]. The second strategy appears particularly intriguing as the electrical response of single molecule magnets (SMMs) depends sensitively on both their spin and charge configuration [7, 8]. This sensitivity, combined with the possibility of manipulating the spin-state of a molecule by electrical means [9, 10], makes spin-electronics based on SMMs an attractive platform for both conventional and quantum logic.

There are however two unfortunate drawbacks in constructing spin-devices based on SMMs. The first concerns with the typically poor structural stability of SMMs away from solution. For instance almost all the molecules in the mostly celebrated  $Mn_{12}$  family react on metallic surfaces, so that one is never certain about their structural and electronic integrity once they are incorporated in a device [11]. The second problem has to do with the magnetic anisotropy. In fact, although the anisotropy density per atom may be very large, the overall magnetic anisotropy of the molecule is usually rather small, since only a handful of atoms contribute to the magnetic moment. This means that at room temperature the spin quantization axis of the molecule fluctuates at a frequency much higher than the transport measurement time and, as such, the molecule appears paramagnetic to a steady state transport experiment. Importantly, while the first problem can be kept under control by engineering the end groups binding the SMM to the substrate [12], the second one appears much more tough to overcome. In fact, quantum tunneling of the magnetization is always present so that the instability in the magnetization direction may persist down to low temperatures, regardless of the anisotropy. It is then not surprising that the only demonstration to date of spin-valve effect orig-

inating from SMM is limited to ultra-low temperatures [13, 14].

One possible way to overcome such a difficulty is to abandon the concept of spin-valve and to look at devices where the information is contained in the actual spin magnitude and not in its direction. A natural choice for such alternative device concept is that of using molecules displaying a magnetic bi-stability, i.e. molecules that can be found in two different spin states, both accessible with an external stimulus. This is the realm of spin-crossover compounds (SCCs) [15]. SCCs are formed by  $3d$  transition metal ions in an octahedral surrounding, which display a spin transition from a low spin state (LS), usually the ground state, to high spin state (HS), usually a metastable one. Such a LS-HS transition can be triggered by temperature, pressure or light irradiation. It is accompanied by a modification of the geometrical structure, which alters the crystal field strength. The most extensively investigated SCCs contain Fe(II) and the transition is between a  $^1A_{1g}$  LS state to a  $^5T_{2g}$  HS one.

To date electron transport experiments in SCCs at the single molecular level remain rather scarce, mostly because the effort in depositing such molecules on surfaces has intensified only recently. However, several deposition techniques are becoming available (e.g. Ref. [16] and references therein) and a first demonstration of light-induced spin-crossover in vacuum-deposited thin films has been already reported [17]. Intriguingly the critical temperature for spin-crossover in such thin films is similar to that of the bulk, giving hope that room temperature device operation may be soon achievable. Also intriguing is the possibility to tune the spin crossover transition with an external electric field, as demonstrated recently for valence tautomeric compounds [18].

Importantly there are two demonstrations of the interplay between the spin-crossover transition and the electron transport properties of a device. Prins *et al.* [19] measured a change in the current-voltage ( $I$ - $V$ ) curve of a  $Fe-(trz)_3$  ( $trz$ =triazole) complex deposited between gold

nano-gap electrodes, which correlates well with the spin-crossover transition. Furthermore, the three-terminal single molecule experiments of Meded *et al.* [20] showed low-energy features attributable to spin-crossover. Most interestingly these can be controlled by gating.

A crucial aspect when investigating the transport properties of SCCs is that at the LS to HS phase transition there is a simultaneous electronic and structural change of the molecule. In particular the electronic gap between the highest occupied molecular orbital (HOMO) and the lowest unoccupied molecular orbital (LUMO) varies accordingly to the different occupation of the  $3d$  multiplet. At the same time there is an out-breathing relaxation of the octahedral cage connected to the weakening of the crystal field. As such, in transport experiments it is difficult to separate effects arising from the electronic structure from those originating simply from the molecule geometry. In this letter we address such an issue with state of the art electron transport calculations based on density functional theory (DFT). In particular we show that the change in HOMO-LUMO gap at the phase transition may generate extremely large changes in the  $I$ - $V$  characteristic. This is demonstrated for the prototypical Fe(II) SCC  $[\text{FeL}_2]^{+2}$ , where  $\mathbf{L}$  is a  $2,2':6,2''$ -terpyridine group [see Fig. 1(a)]. Note that qualitatively similar results (not presented here) have been obtained for a second  $[\text{FeL}_2]^{+2}$  compound where  $\mathbf{L} = 2,6\text{-bis(pyrazol-1-yl)}$ , so that we expect our main conclusions to bare generality.

Calculating the electronic properties of SCCs with DFT is a rather difficult task as the relative energy separating the LS and HS state is very sensitive to the choice of exchange and correlation functional and to the atomic relaxation [21] (note that the atomic coordinates of a given molecule are known only for single crystals but not in vacuum or on a surface). We then use the following strategy. We first perform structural relaxation for the molecule in vacuum by using the B3LYP functional [22], one of the better performing for this problem. Then the results are compared with those obtained by using the generalized gradient approximation (GGA) and the local density approximation incorporating the self-interaction corrections (LDA-ASIC) [23]. From this analysis we select the GGA functional to be used for the electron transport calculations, as this reproduces qualitatively the B3LYP HOMO-LUMO gap [24].

We start our analysis by discussing the electronic and geometric properties of the molecule in the gas phase. B3LYP calculations are performed with the NWChem package [25]. The basis set is 6-31++G\*\* for H, C and N, while for Fe we use the Los Alamos double zeta (LANL2DZ) with an effective core potential (ECP) [26]. In Fig. 1(c) we present the total energy as a function of the reaction coordinates,  $X$ , interpolating between the LS ( $X = 0$ ) and the HS ( $X = 1$ ) geometry for the two different spin configurations. In the same figure we also show the dependence of the B3LYP HOMO-LUMO gap,

$\Delta E_g$ , of the two spin states as a function of  $X$ .

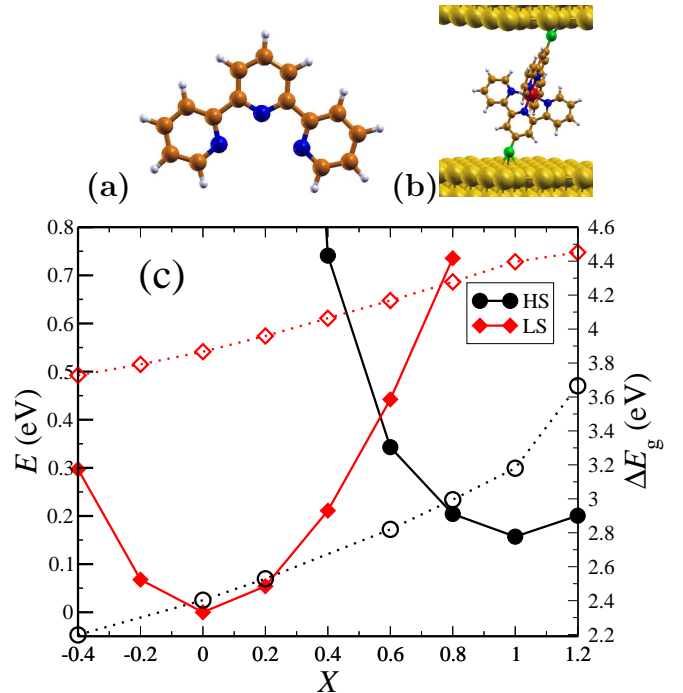


FIG. 1: (Color on line) Electronic properties of  $[\text{FeL}_2]^{+2}$ ,  $\mathbf{L} = 2,2':6,2''$ -terpyridine, along the reaction coordinates,  $X$ . In (a) and (b) we show respectively the  $2,2':6,2''$ -terpyridine group and the cell used for the transport calculations. Color code: C=orange, N=dark blue, H=white, S=green and Au=yellow. In panel (c) we present the total energy,  $E$  (full symbols to read on the left-hand side scale), and the B3LYP HOMO-LUMO gap,  $\Delta E_g$  (open symbols to read on the right-hand side scale), for both LS and HS along  $X$ .

The figure clearly shows that the ground state is the expected LS. As  $X$  increases there is a transition to HS for  $X \sim 0.6$  and the difference between the LS and HS energy minima is about 200 meV. The HOMO-LUMO gap also changes as a function of the reaction coordinates increasing for both the spin states as one goes from the LS to the HS geometry ( $X$  gets bigger), i.e. as the ligand field weakens. Most importantly at the relative energy minimum the B3LYP gap of the LS state is 3.87 eV (for  $X=0$ ), while that of the HS is only 3.18 eV (for  $X=1$ ). At the same two energy minima LDA-ASIC (with scaling parameter  $\alpha = 0.7$ ) gives us HOMO-LUMO gaps of 3.35 eV (LS) and 2.84 eV (HS), while GGA returns 1.81 eV (LS) and 0.33 eV (HS). Although different exchange and correlation functionals yield sensibly different HOMO-LUMO gaps, in all cases this contracts significantly across the phase transition. Importantly both B3LYP and GGA give us spin down,  $\downarrow$ , HOMO and LUMO levels in the HS state, while with LDA-ASIC the HOMO is a spin up,  $\uparrow$ , state and the LUMO is  $\downarrow$ . As such, we decide to use

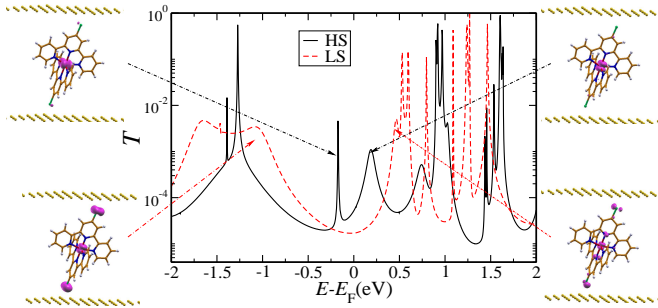


FIG. 2: (Color on line) Zero-bias transmission coefficient as a function energy,  $T(E; V = 0)$ , for both the LS (red dashed line) and the HS (solid black line) configuration of the  $\text{FeL}_2$ -based junction and the molecular orbitals associated to their HOMO and LUMO like-orbital. Calculations are performed with the GGA functional.

GGA instead of LDA-SIC for the transport calculations, which are presented next.

We construct a two terminal device by attaching the  $\text{FeL}_2$  molecule to a Au(111) surface via thiol group. In particular we consider here bonding to the (111) hollow site and we optimize the Au-S distance for two different angles between the molecule and the normal to the surface, namely 0 and  $30^\circ$ . As the differences in transport through the LS and the HS state of the molecule depend weakly on such tilting angle the results reported here refer only to the  $30^\circ$  case. This is the bonding geometry presenting a lower energy. Transport calculations are performed with the *Smeagol* code [27, 28], which implements the non-equilibrium Greens function method within DFT. *Smeagol* uses the *Siesta* package [29] as DFT engine, so that the wave-function is expanded over a numerical atomic orbital basis set and the core electrons are described with norm-conserving pseudopotentials including non-linear core corrections. In particular we consider here a basis set of double zeta quality for C, N, H and Fe, while only single zeta is employed for Au. The simulation cell for the transport calculation contains, in addition to the molecule, 5 (111)-oriented Au layers with  $8 \times 7$  cross section. We use periodic boundary conditions in the direction orthogonal to the transport with a uniform  $2 \times 2$   $k$ -point sampling and an equivalent mesh cutoff of 400 Ry. The charge density is integrated over 64 energy points along the semi-circle, 64 energy points along the line in the complex plane and 64 poles are used for the Fermi distribution (the electronic temperature is 25 meV). During the finite-bias calculations we integrate the Green's function over the real axis on a 256 point mesh.

Figure 2 displays the total zero-bias transmission coefficient,  $T(E; V = 0) = \sum_{\sigma}^{\uparrow\downarrow} T^{\sigma}(E; V = 0)$ , as a function of energy for both the LS and HS configurations of the junction ( $\sigma$  labels the spin). The most striking feature is

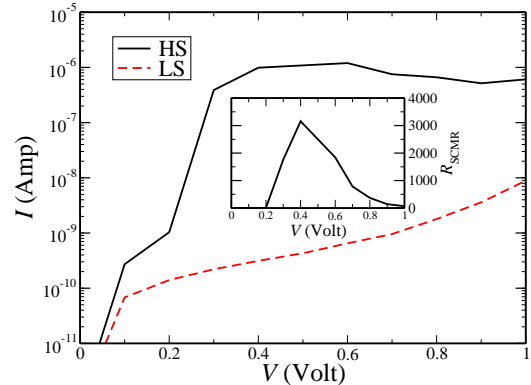


FIG. 3: (Color on line)  $I$ - $V$  curve for a  $\text{FeL}_2$  molecule attached to gold electrodes in either the HS (black solid line) or the LS (red dashed line) state. The current is plotted on a logarithmic scale only for positive currents. The inset shows the spin-crossover magneto-resistance (SCMR) ratio,  $R_{\text{SCMR}}$ . All calculations are at the GGA level.

a radical change of the position of the various resonant peaks as the molecule transits from LS to HS. This is a direct consequence of the re-arrangement of the Fe  $d$  shell density of state (DOS) originating from the reduction of the ligand crystal field. In particular as the crystal field weakens in the HS state the energy width of  $d$ -shell reduces and the peaks become more dense. This effect is particularly dramatic around the Fermi level,  $E_F$ , where the transport HOMO-LUMO gap shrinks. Recalling here the fact that in the linear response the conductance  $G$  is simply given by  $G = \frac{e^2}{h} T(E_F; V = 0)$ , we can conclude that at the phase transition there is a significant conductance enhancement. One can quantify such an effect by defining the spin-crossover magneto-resistance (SCMR) ratio as  $R_{\text{SCMR}} = (G_{\text{HS}} - G_{\text{LS}})/G_{\text{LS}}$ . In the present case at zero-bias we find  $R_{\text{SCMR}} = 200\%$ , a variation which is certainly measurable.

Some more details are provided by the insets of Fig. 2, where we show the frontier molecular orbitals associated to the different peaks in  $T(E; V = 0)$ . In general around the Fermi level the orbitals responsible for the transmission have all Fe- $d$  character and present little mixing with the ligands. In the LS configuration the HOMO and LUMO are non-spin-polarized and have respectively  $d_{z^2}$  and  $d_{\pi}$  character. In contrast the HS state has a HOMO of  $x^2 - y^2$  symmetry, while the LUMO is  $d_{\sigma}$ -like, but both the HOMO and the LUMO are spin down. Thus the gap reduction is the result of the orbital re-arrangement of the  $d$  manifold associated to the spin crossover transition. In the LS state the gap is between the  $t_{2g}$  triplet and  $e_g$  doublet split by the octahedral crystal field. In the HS configuration the system undergoes Jahn-Teller distortion in the singly occupied spin down triplet (the spin up is fully occupied) and thus the gap reduces.

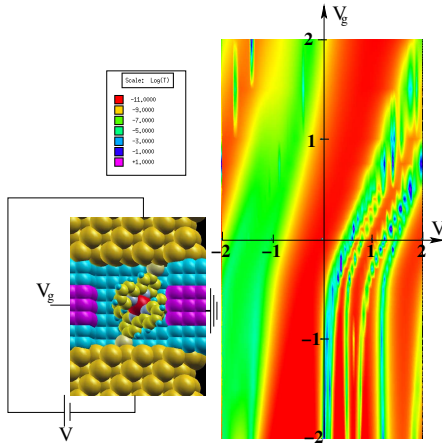


FIG. 4: (Color on line) Transmission coefficients as a function of energy for different values of the gate potential  $V_g$ . Here  $T(E; V = 0)$  is plotted as a color code on a logarithmic scale with red corresponding to low transmission ( $10^{-11}$ ) and blue to high ( $10^{-1}$ ). In the inset we show a schematic figure of the device investigated. The purple atoms represent the region in space where the gate is applied. The color code for the atoms is the same as in Fig. 1(b).

Then we look at the current-voltage,  $I$ - $V$ , characteristics of the junction when the molecule is in either its LS or HS configuration. The results are presented in Fig. 3. Clearly, the drastic gap reduction in the HS state makes its relative current considerably larger than that of the LS one and, for instance, at a voltage of about 0.5 Volt the two differ by more than three orders of magnitude. The LS current is essentially tunneling-like over the entire bias window investigated and it increases monotonically with bias. Such an increase is the result of the enlargement of the bias window, i.e. of the fact that a larger portion of the transmission spectrum contributes to the current. It is then the tail of the LUMO which contributes the most. The HS situation is different since voltages of the order of 0.4 Volt are enough for bringing both the HOMO and the LUMO transmission resonances within the bias window (note that orbital re-hybridization under bias drifts both the HOMO and LUMO close to each other hence decreasing the gap). As a consequence the current grows fast at low bias when there is a transition from tunneling to resonant transport and then saturates. Such a large difference in the  $I$ - $V$  characteristics of the two molecule spin states translates in a large  $R_{\text{SCMR}}$ , which is presented as a function of bias in the inset of Fig. 3. Clearly  $R_{\text{SCMR}}$  as large as 3000% appear possible.

Finally, we look at the effect of a potential gate on the transport properties of the molecule. We note that for both states the transmission spectrum is characterized by a number of relatively sharp peaks spaced by at most 1.5 eV (most typically the spacing is  $\sim 0.3$  eV) and corresponding to states with substantial Fe  $d$  character.

These are expected to shift with bias. As an example we consider the LS situation and in figure 4 we show  $T(E; V = 0)$  as a function of gate. Here  $T$  is plotted as a color code on a logarithmic scale with red corresponding to low transmission ( $10^{-11}$ ) and blue to high ( $10^{-1}$ ). Clearly the entire spectrum shifts with the gate potential until a state, either the HOMO or the LUMO, crosses the Fermi level ( $V = 0$ ). At that point charge transfer takes place and the gate becomes less efficient. Crucially when one of the two frontier molecular orbitals is brought to  $E_F$  the zero-bias conductance increases dramatically. Since the two spin states of the molecule have different frontier molecular orbitals, their position can be manipulated independently, i.e. they can be brought at  $E_F$  for different values of the gate. As such, an extremely large gate-modulated magnetoresistance is expected.

In conclusion we have demonstrated that the changes in electronic structure associated to the spin crossover phase transition, namely the reduction of the HOMO-LUMO gap, produce large changes in the transmission of a two-terminal molecular junction. At low bias we have predicted a magnetoresistances of the order of 200%, which can increase up to 3000% at finite bias. The effect is related to the different nature of the frontier molecular orbitals of the different spin configurations and can be tuned with a gate potential. Such an effect, whose experimental evidence has been already partially provided, can be exploited in the fabrication of spin-transistors at the molecular level.

This work is supported by Science Foundation of Ireland under the NanoSci-E+ project “Internet” (08/ERA/I1759).

---

- [1] S. Sanvito, Chem. Soc. Rev. **40**, 3336 (2011).
- [2] L. Bogani and W. Wernsdorfer, Nature Mater. **7**, 179 (2008).
- [3] S. Sanvito, J. Mater. Chem. **17**, 4455 (2007).
- [4] J.R. Petta, S.K. Slater and D.C. Ralph, Phys. Rev. Lett. **93**, 136601 (2004).
- [5] A. R. Rocha, V. Garcia Suarez, S. W. Bailey, C. J. Lambert, J. Ferrer and S. Sanvito, Nature Mater. **4**, 335 (2005).
- [6] C. Barraud, P. Seneor, R. Mattana, S. Fusil, K. Bouzehouane, C. Deranlot, P. Graziosi, L. Hueso, I. Bergenti, V. Dedi, F. Petroff and A. Fert, Nature Phys. **6**, 615 (2010).
- [7] H. B. Heersche, Z. de Groot, J. A. Folk, H. S. J. van der Zant, C. Romeike, M. R. Wegewijs, L. Zobbi, D. Barreca, E. Tondello and A. Cornia, Phys. Rev. Lett. **96**, 206801 (2006).
- [8] C.D. Pemmaraju, I. Rungger and S. Sanvito, Phys. Rev. B **80**, 104422 (2009).
- [9] J. Lehmann, A. Gaita-Arino, E. Coronado and D. Loss, Nature Nanotech. **2**, 312 (2007).
- [10] N. Baadji, M. Piacenza, T. Tugsuz, F. D. Sala, G. Maruccio and S. Sanvito, Nature Materials **8**, 813 (2009).

- [11] M. Mannini, P. Sainctavit, R. Sessoli, C. Cartier dit Moulin, F. Pineider, M.-A. Arrio, A. Cornia and D. Gatteschi, *Chem. Eur. J.* **14**, 7530 (2008).
- [12] M. Mannini, F. Pineider, C. Danieli, F. Totti, L. Sorace, P. Sainctavit, M.A. Arrio, E. Otero, L. Joly, J. C. Cezar, A. Cornia and R. Sessoli, *Nature* **468**, 417 (2010).
- [13] M. Urdampilleta, et al. *Nature Materials* **10**, 502 (2011).
- [14] S. Sanvito, *Nature Materials* **10**, 484 (2011).
- [15] P. Gütlich, H.A. Goodwin, in *Spin Crossover in Transition Metal Compounds* (eds. P. Gütlich, H.A. Goodwin) (Springer, 2004).
- [16] S. Shi et al., *Appl. Phys. Lett.* **95**, 043303 (2009).
- [17] H. Naggert, A. Bannwarth, S. Chemnitz, T. von Hofe, E. Quandt and F. Tuczek, *Dalton Trans.* **40**, 6364 (2011).
- [18] A. Droghetti and S. Sanvito, *Phys. Rev. Lett.* **107**, 047201 (2011).
- [19] F. Prins, M. Monrabal-Capilla, E.A. Osorio, E. Coronado and H.S.J. van der Zant, *Adv. Mat.* **23**, 1545 (2011).
- [20] V. Meded et al., *Phys. Rev. B* **83**, 245415 (2011).
- [21] S. Zein, S.A. Borshch, P. Fleurat-Lessard, M.E. Casida, H. Chermette, *J. Chem. Phys.* **126**, 014105 (2007).
- [22] A.D. Becke, *J. Chem. Phys.* **98**, 5648 (1993).
- [23] C.D. Pemmaraju, T. Archer, D. Sánchez-Portal and S. Sanvito, *Phys. Rev. B* **75**, 045101 (2007).
- [24] Note that our electron transport code *Smeagol* at present cannot use non-local functionals. Furthermore in general, as far as we know, an implementation of hybrid functions within the non-equilibrium Green's function formalism has not been developed yet.
- [25] M. Valiev et al., *Computer Phys. Comm.* **181**, 1477 (2010).
- [26] P. J. Hay and W. R. Wadt, *J. Chem. Phys.* **82**, 299 (1985).
- [27] A.R. Rocha et al., *Phys. Rev. B* **73**, 085414 (2006); A.R. Rocha et al., *Nature Materials* **4**, 335 (2005).
- [28] I. Rungger and S. Sanvito, *Phys. Rev. B* **78**, 035407 (2008).
- [29] J.M. Soler et al., *J. Phys.: Condens. Matter* **14**, 2745 (2002).